

Case Report

Spontaneous bilateral thyroid follicular cell carcinoma (subtype: compact cellular carcinoma) with C-cell complexes in a male beagle

Shingo Miyazaki^{1*}, Takashi Ogawa¹, Tomoya Onozato¹, Yuji Okuhara¹, Tatsuya Nagasawa¹, and Morimichi Hayashi¹

¹ Safety Research Laboratory, Kissei Pharmaceutical Co., Ltd., 2320-1 Maki, Hotaka, Azumino, Nagano 399-8305, Japan

Abstract: We report the features of spontaneous bilateral thyroid follicular cell carcinoma in a 10-year-old male beagle. Necropsy revealed bilateral masses on the trachea, corresponding to the left and right sides of the thyroid gland. The masses were elastic, encapsulated, and distinct, with no connecting tumor tissues between them. Histologically, the tumor cells exhibited a predominant sheet-like growth pattern in both masses, and small follicular structures containing colloid were observed. Immunohistochemically, >50% of the tumor cells were positive for thyroglobulin. In the sheet-like growth area, all tumor cells were positive for cytokeratin and approximately 50% of them were positive for vimentin. The tumor cells were negative for calcitonin and parathormone. Electron microscopy of the tumor cells revealed colloid droplets and lysosomes in the cytoplasm, which are characteristics of follicular cells of the thyroid gland, although they were abnormally shaped and smaller in size compared to the normal cells. Many calcitonin-positive C cells were observed in the nodule area without a capsule in the left mass and were scattered within the tumor in the right mass. C cells were found individually and were negative for Ki-67 expression. Therefore, each of these cells was deemed to be derived from an individual C-cell complex. Based on these morphological features, the tumor was diagnosed as spontaneous bilateral thyroid follicular cell carcinoma of the compact cellular carcinoma subtype. This is the first report of electron microscopic findings and co-expression of cytokeratin and vimentin in thyroid follicular cell carcinoma in beagles. (DOI: 10.1293/tox.2024-0072; J Toxicol Pathol 2025; 38: 83–91)

Key words: beagles, thyroid glands, follicular cell carcinoma, compact cellular carcinoma, C-cell complex

Thyroid tumors account for 1.1% of all tumors in dogs, of which 90% are diagnosed as malignant¹. Ninety percent of cases occur in dogs aged 7 years or older, and the incidence is reported to be higher in beagles than in other dog breeds^{1,2}. The number of cases where they occur bilaterally ranges from 20% to 60%^{3,4}. Despite its high incidence, there are few reports on the histological, immunohistochemical, and ultrastructural features of bilateral thyroid carcinoma in beagles. In addition, among thyroid tumors, it is often difficult to differentiate follicular cell carcinoma of compact cellular (solid) carcinoma subtype, C-cell (medullary) carcinomas, and parathyroid carcinomas using the HE staining technique alone because they have similar cell morphologies and sheet-like growth patterns. Therefore, immunohistochemical examination is often required to distinguish these tumors^{1–7}.

Herein, we report the histological, immunohistochemi-

cal, and ultrastructural features of spontaneous bilateral thyroid follicular cell carcinoma of the compact cellular carcinoma subtype in a 10-year-old male beagle. In this case, it was difficult to differentiate the tumors from the C-cell carcinomas because of the presence of many calcitonin-positive C cells, which were deemed to be derived from existing C-cell complexes.

A male beagle was obtained from Marshall BioResources (North Rose, NY, USA) for new drug candidate evaluations conducted in compliance with our institutional guidelines, which conform to the Guide for the Care and Use of Laboratory Animals (Eighth Edition) and current Japanese regulations. All experiments were approved by the Laboratory Animal Care and Use Committee of the Central Research Laboratory, Kissei Pharmaceutical Co., Ltd. This animal has been used in several drug studies, none of which have been considered to cause thyroid carcinoma. The animal was euthanized and necropsied at 10 years of age because of hematuria and decreased activity. Necropsy revealed bilateral masses (left: 35 × 32 × 20 mm; right: 40 × 30 × 28 mm) on the left and right sides of the trachea, corresponding to the thyroid glands. Both the masses were elastic and covered in a capsule with no bilateral continuity. The cut surfaces of both formalin-fixed masses were grayish-white to yellowish-brown and were partially demarcated by connective tissue (Fig. 1). The time of occurrence of the masses was unknown because the neck was not palpated

Received: 23 August 2024, Accepted: 26 October 2024

Published online in J-STAGE: 13 November 2024

*Corresponding author: S Miyazaki

(e-mail: shingo_miyazaki@pharm.kissei.co.jp)

©2025 The Japanese Society of Toxicologic Pathology

This is an open-access article distributed under the terms of the Creative Commons Attribution Non-Commercial No Derivatives

(by-nc-nd) License. (CC-BY-NC-ND 4.0: <https://creativecommons.org/licenses/by-nc-nd/4.0/>).



while the animal was alive. Both masses were fixed in 10% phosphate-buffered formalin, embedded in paraffin, cut into 3 μ m sections, and stained with hematoxylin-eosin (HE) for microscopic examination. Pathological examination of other organs revealed urothelial carcinoma of the bladder, which was determined to be the cause of hematuria. Blood and genetic tests were not performed during necropsy. Additional histochemical staining, including direct fast scarlet for amyloid and Masson's trichrome (MT) staining, was performed. Immunohistochemical staining was performed using the EnVision™ + Dual Link System-HRP kit (Dako A/S, Glostrup, Denmark) and antibodies against thyroglobulin, calcitonin, parathormone, cytokeratin AE1/AE3 (CK), vimentin, and Ki-67. The sources and clones of these antibodies and the results of immunohistochemical staining are shown in Table 1. For electron microscopy, pieces of formalin-fixed tissue from both tumors were immersed in half-strength Karnovsky's solution and fixed using 1% osmium tetroxide. Ultrathin sections were stained with uranyl acetate and lead citrate and evaporated with carbon.

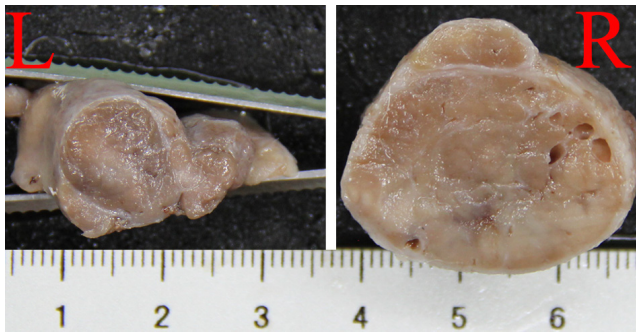


Fig. 1. Cross-sectional gross appearance of the formalin-fixed grayish-white to yellowish-brown masses in the left (L) and right (R) lobes of the thyroid gland in a male beagle.

In addition, the thyroid gland of an untreated normal male 4-year-old beagle, previously kept at the same facility, was prepared in the same manner as the control specimen. The specimens were observed using a transmission electron microscope (JEM-1400Flash, JEOL Ltd., Tokyo, Japan).

The left and right masses were both tumors and showed common characteristics but had different histological features (Figs. 2 and 3). The left tumor was covered in a thick fibrous capsule and consisted of a broad central area and adjacent nodular areas which were divided by fibrous tissue (Fig. 2a). No normal thyroid follicles were observed and most of the tissue was replaced with tumor cells. The growth pattern of the tumor cells was predominantly sheet-like with fibrous tissue and microvessels running between them (Fig. 2b). Small follicular structures with eosinophilic colloid-like substances were observed in the lumen in some areas (Fig. 2c). The tumor cells were pleomorphic with well-defined to slightly indistinct cell borders and broad and weakly eosinophilic foamy cytoplasm. The nuclei were round to oval in shape with poor chromatin content and many contained a single distinct nucleolus. In addition, one nodular area was not covered with a capsule and contained many single C cells with eosinophilic and fine granular cytoplasm (Fig. 2d). In the parathyroid gland at the tumor margin, the tumor cells infiltrated and proliferated in the center, and normal parathyroid cells were compressed at the periphery.

Similar to the left tumor, the right tumor was covered in a thick fibrous capsule and normal large follicles were replaced by tumor cells (Fig. 3a). Many large blood vessels were also observed. There were dense areas with sheet-like areas or cords of tumor cells similar to the left tumor and sparse areas in which tumor cells formed small follicles or island-like nests with abundant weakly eosinophilic fibers or mucus-like material and microvessels in the stroma (Fig. 3b and 3c). In the dense area, the morphological features of the tumor cells were similar to those of the left tu-

Table 1. Immunohistochemistry Antibodies and Results of Staining

Antibody	Manufacturer	Host species	Clonality (clone name)	Dilution ratio	Antigen retrieval method (treatment solution)	Results			
						Tumor cells		C cells	Parathyroid cells
						Sheet-like growth area	Follicle growth area		
Thyroglobulin	Dako	Rabbit	Polyclonal (2H11)	Ready to use	Not applicable	+++ --	+++	–	–
Calcitonin	NOVUS	Rabbit	Monoclonal (SP17)	1 : 500		–	–	+++	–
Parathormone	Abcam	Mouse	Monoclonal (D1.1)	1 : 500		–	–	–	+++
Cytokeratin AE1/AE3	Dako	Mouse	Monoclonal (AE1/AE3)	Ready to use	Microwave, 15 min (Dako Target retrieval Solution)	+++ -- +	+++	+++	+
Vimentin	Dako	Mouse	Monoclonal (V9)	Ready to use		+++ --	–	–	–
Ki-67	Abcam	Rabbit	Monoclonal (SP6)	1 : 500		–	–	–	–
						Only a few cells: +++			

Immunohistochemical staining intensity: negative (–), slightly positive (+), and strongly positive (+++).

mor, but some tumor cells were larger and had a slightly clearer cytoplasm (Fig. 3d). No parathyroid cells were observed in the right tumor in the sections examined in this study. In the dense area, C cells were scattered over a wide area (Fig. 3e). Red blood cells were also observed in sparse areas. Capsular and vascular invasion was observed in both the left and right tumors, but almost no mitotic figures were observed in the tumor cells.

In this case, bilateral masses were observed but there was no bilateral continuity. On histopathological examination, it was impossible to determine whether the tumor was primary or metastatic. Considering that the tumors were bilateral, the pituitary gland may have been affected; however, we did not have a pituitary gland specimen from this animal to confirm this. Although capsular and vascular infiltration was observed, no metastasis was observed, even in the lungs, which are the most common metastatic organ⁵. Therefore, the metastatic potential was low, and together with the lack of bilateral continuity, the left and right tumors were likely to have occurred separately.

The results of direct fast scarlet staining for amyloid, MT staining, and immunostaining were similar for both the left and right tumors (Table 1). Immunostaining showed that the tumor cells in the follicular island-like growth area and most of the tumor cells in the sheet-like growth area were positive for thyroglobulin, whereas the tumor cells in the center of the sheet-like area and those with a large and partially clear cytoplasm in the right tumor were negative (Fig. 4a, 4b, and 4c). Tumor cells in the sheet-like area were positive for cytokeratin AE1/AE3 and approximately 50% were positive for vimentin (Fig. 5a and 5c). Tumor cells that formed small follicles in the right tumor were positive for cytokeratin AE1/AE3, but negative for vimentin (Fig. 5b and 5d). Microvessels and fibroblasts in the stroma were also positive for vimentin. The C cells were positive for calcitonin (Fig. 6), and the parathyroid cells in the left tumor were positive for parathormone. Only a few tumor cells were positive, and C cells were negative for Ki-67 in both the tumors. MT staining revealed that colloids formed by small follicular tumor cells were stained blue to red, stro-

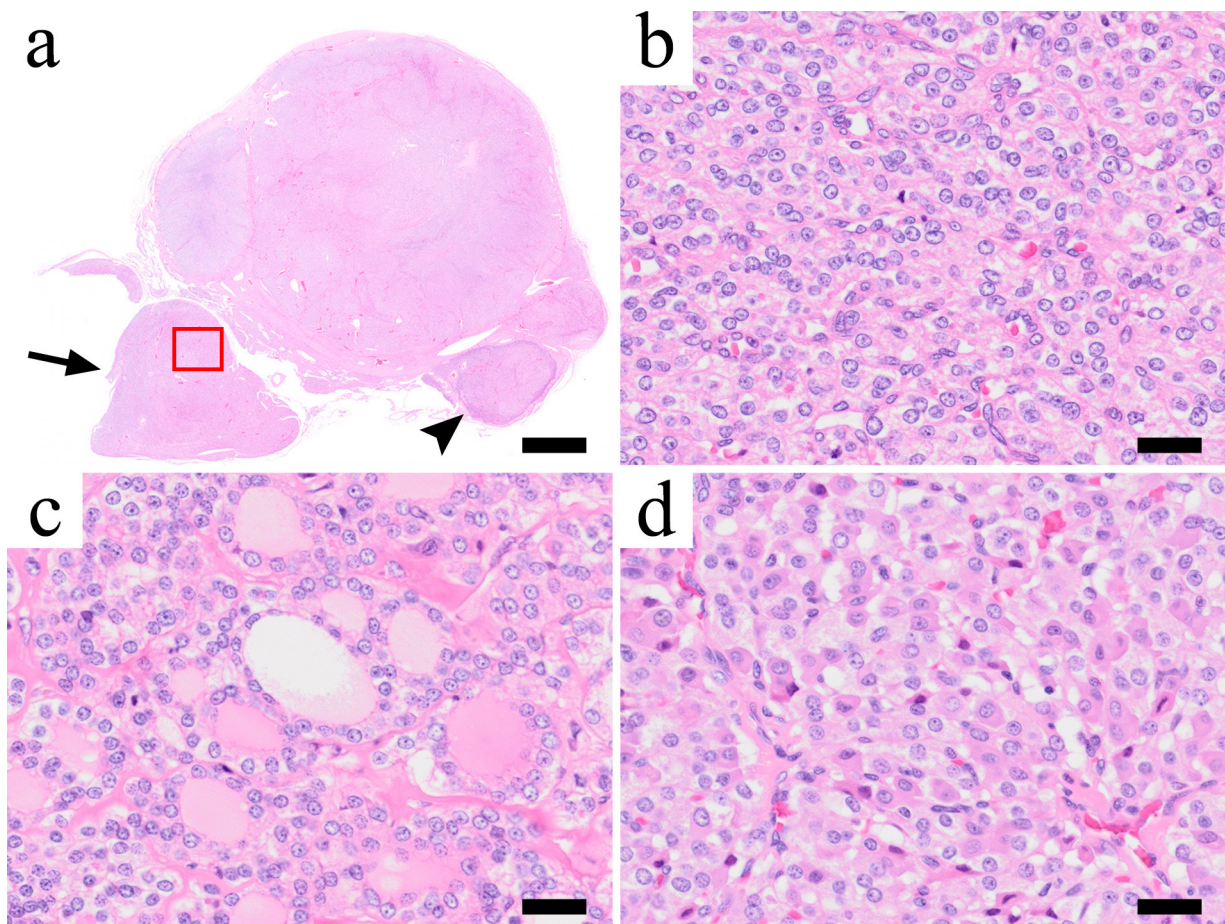


Fig. 2. Histological appearance of the left tumor. a) Loupe image of the left tumor. The left mass was covered with a thick fibrous capsule. However, no capsule was observed in the nodule area indicated by the arrow. In the parathyroid gland indicated by the arrowhead, the tumor cells had infiltrated and proliferated in the center, and the normal parathyroid cells were compressed at the periphery. b) Sheet-like growth area. c) Follicular growth area. d) C cells in a sheet-like growth area surrounded by the square indicated in (a). HE staining. Bars=2 mm (a) and 25 μ m (b, c, and d).

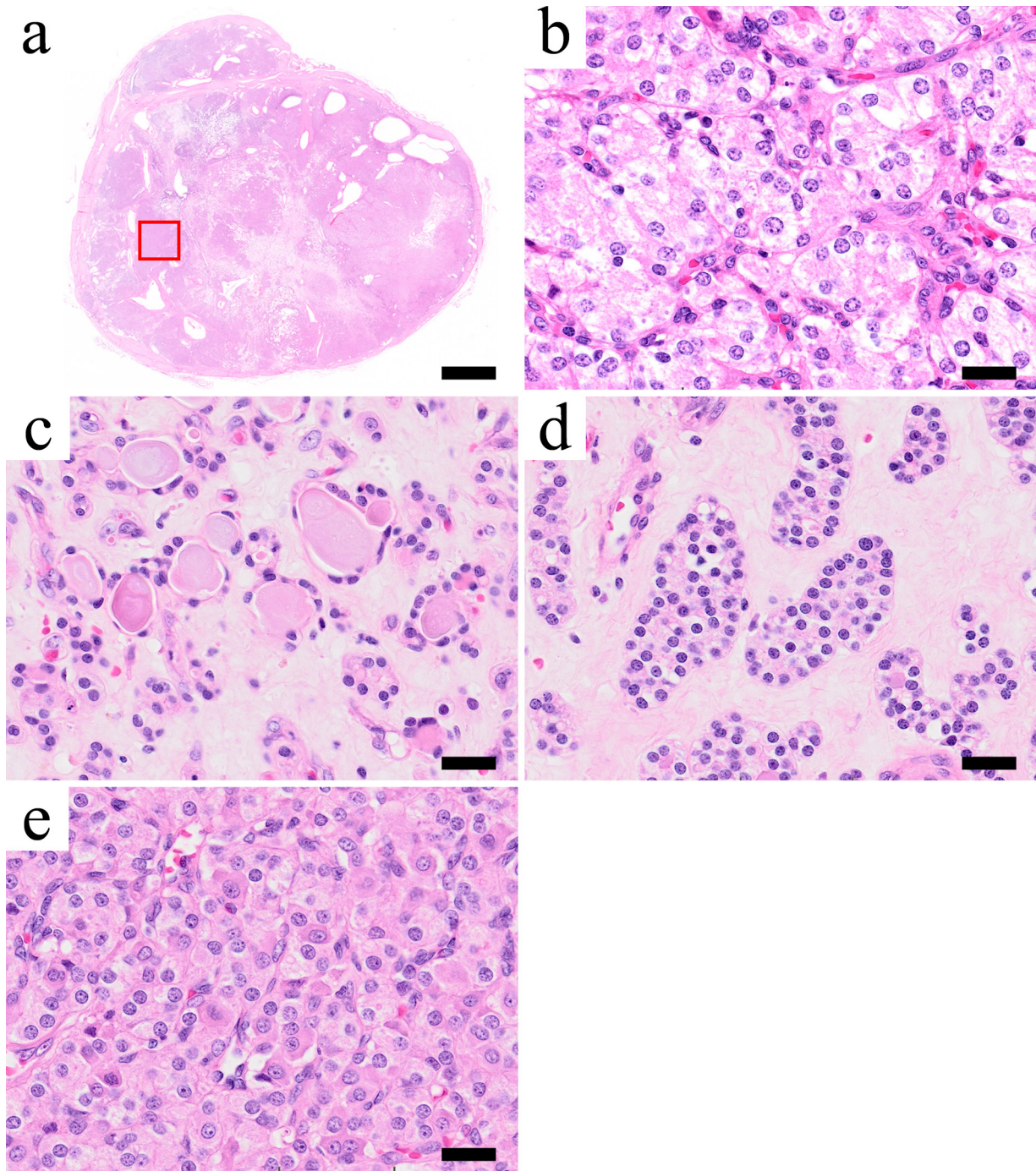


Fig. 3. Histological appearance of the right tumor. a) Loupe image of the right tumor. The right mass was covered with a thick fibrous capsule. b and c) Follicular and island-like growth areas with abundant weak eosinophilic fibers or mucus-like materials. d) Sheet-like growth area. The tumor cells are large and have partially clear cytoplasm. e) C cells in a sheet-like growth area surrounded by the square indicated in (a). They were scattered over a wide area. HE staining. Bars=3 mm (a) and 25 μ m (b, c, d, and e).

mal fibers were stained blue, and fibers or myxoid material in sparse areas of the right tumor were stained pale blue (Fig. 4d). Amyloid staining results were negative.

Electron microscopy revealed colloid droplets and lysosomes in the cytoplasm of tumor cells, which are characteristic of follicular cells of the thyroid glands, although they were irregularly shaped or small compared to those in

the normal cells (Fig. 7)^{8,9}. Colloid droplets and lysosomes were also observed in thyroglobulin-negative tumor cells with a large and partially clear cytoplasm (Fig. 7e and 7f).

In this case, it was difficult to differentiate the tumors from C-cell carcinoma because of the presence of many calcitonin-positive C cells in one nodule in the left tumor and relatively extensive C cells in the right tumor (Fig. 6). These

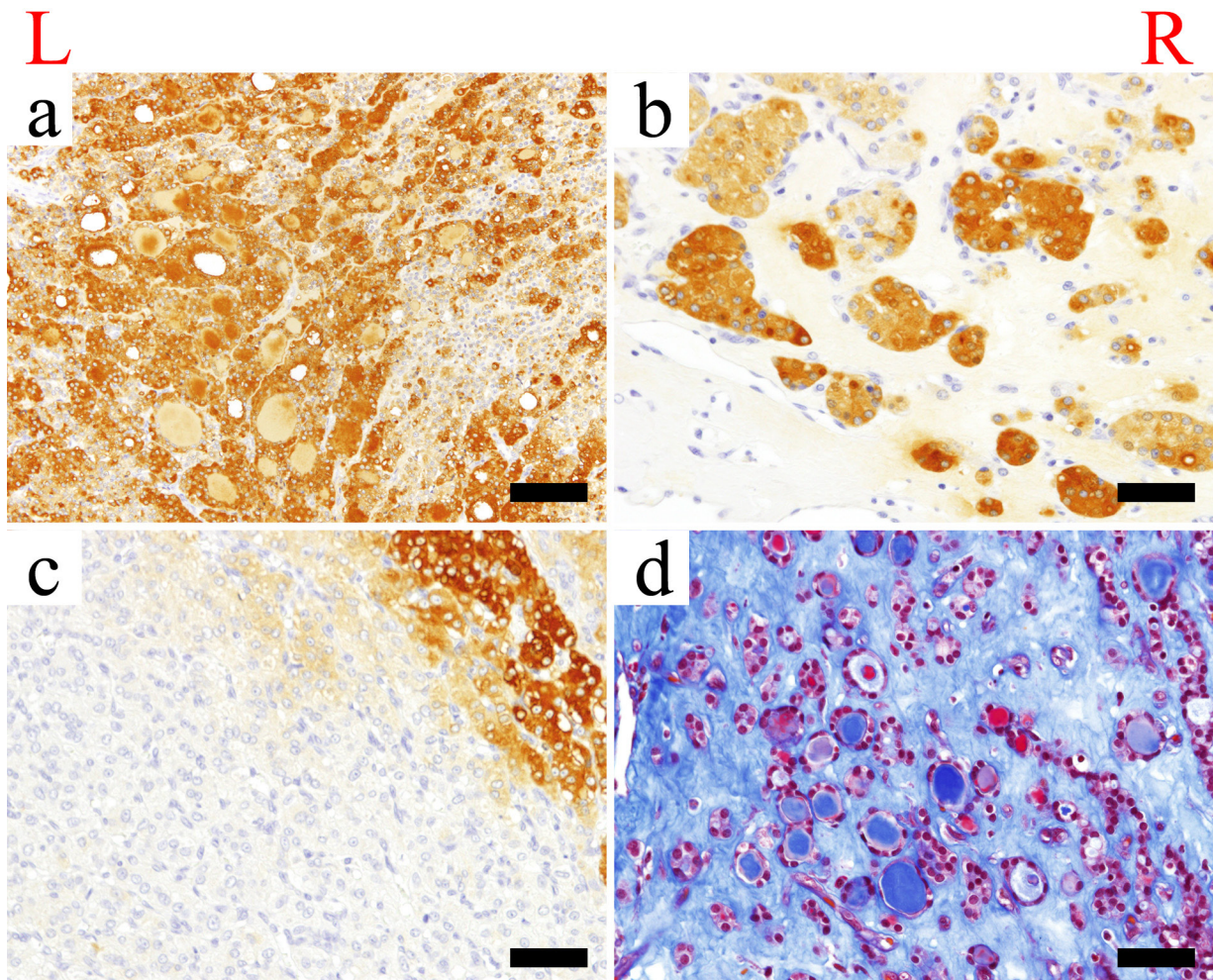


Fig. 4. Immunohistochemical staining for thyroglobulin (a–c) and MT (d) staining. a and c) Left tumor. b and d) Right tumor. Tumor cells were positive for thyroglobulin in the follicular (a) and island-like (b) growth areas, but were negative in the central sheet-like growth area (c). d) MT staining showed blue to red colloids in the follicular growth area and pale blue fibrous or plasma components in the stroma. Bars=100 μ m (a) and 50 μ m (b, c, and d).

C cells were deemed to be derived from the existing C-cell complexes. The C-cell complex in dogs is an aggregate of many C cells derived from ultimobranchial bodies arising from the fourth pharyngeal pouch, follicular cells, and undifferentiated epithelial cells at various developmental stages¹⁰. Such complexes can be observed in intra- and extra-thyroidal tissue with no fibrous capsule near parathyroid gland IV in approximately 65% of dogs^{10–13}. In this case, all C cells in both tumors were solitary without forming clusters and were negative for Ki-67; therefore, we considered them to be C cells rather than tumor cells. Furthermore, the fact that the C cells in the left tumor were mainly observed in one nodule that did not have a capsule and was separated from the main tumor region suggested that they were C-cell complexes (Fig. 2a). However, the calcitonin-positive C cells in the tumor were well differentiated and considered distinct from the C-cell complexes, which are aggregates of C cells at various developmental stages and undifferentiated epithelial cells. However, considering that the differentia-

tion of both follicular cells and C cells in the C-cell complexes progresses with age and that this animal was 10 years old, was not inconsistent with our conclusion. With respect to the thyroglobulin-positive cells in one nodule without a capsule in the left tumor, we considered that the tumor cells had infiltrated the C-cell complexes because their morphology was undifferentiated, and almost no follicular structure was observed. In the right tumor, unlike the left tumor, C cells were widely observed in the sheet-like growth area. We considered three possible reasons for this: dispersion of C-cell complexes due to tumor cell infiltration, the presence of multiple C-cell complexes, and the tumor derived from a C-cell complexes. However, it was difficult to determine why C cells were present in the sheet-like areas. Due to the presence of many C cells, mixed medullary-follicular thyroid carcinoma (MMFTC) was also considered. However, the diagnosis of MMFTC requires both follicular and C cells; therefore, MMFTC was ruled out because no proliferation of C cells was observed^{1, 2, 5, 14–16}.

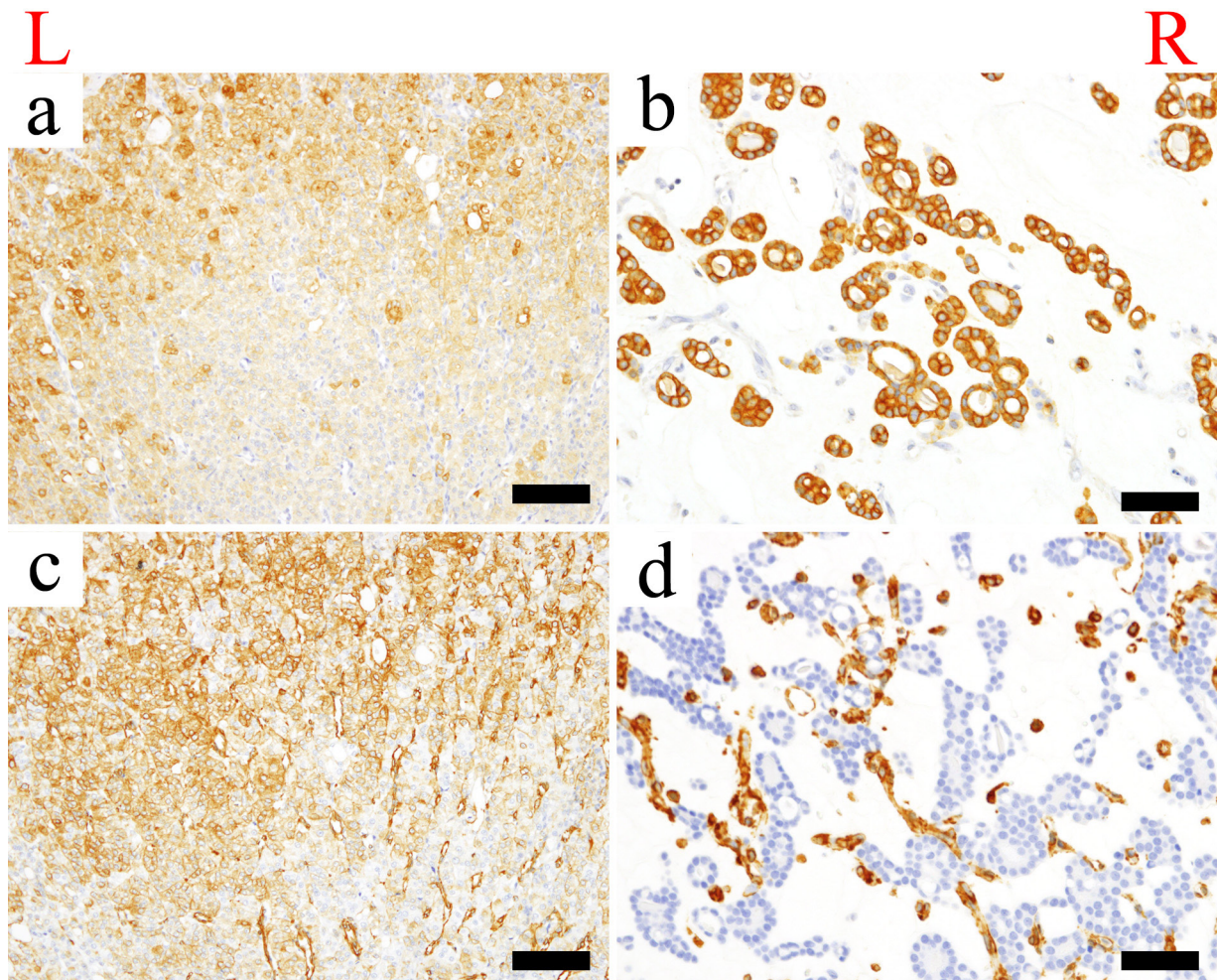


Fig. 5. Immunohistochemical staining for cytokeratin AE1/AE3 (a and b) and vimentin (c and d). a and c) Left tumor. Tumor cells in the sheet-like growth area were positive for both cytokeratin AE1/AE3 and vimentin. b and d) Right tumor. Tumor cells in the follicular growth area were positive for cytokeratin AE1/AE3 but negative for vimentin. Stromal microvessels were positive for vimentin. Bars=100 μ m (a and c) and 50 μ m (b and d).

The tumor cells in the sheet-like growth area were positive for CK and approximately 50% of them were positive for vimentin. Vimentin filaments in thyroid follicular cells may participate in thyroglobulin synthesis and folliculogenesis¹⁰. It has been reported that the expression of vimentin in follicular cells is positive in immature follicular cells that do not form follicles, small follicles, or follicular cells that do not have colloids in the lumen, but negative in typical follicular cells that form expanded follicles and contain colloids^{10, 12}. Concerning the expression of CK and vimentin in thyroid carcinoma, it has been reported that vimentin is expressed in dogs and both are expressed in humans^{17, 18}. In this case, the tumor cells maintained intercellular junctions and showed a sheet-like growth pattern; no spindle-shaped tumor cells were observed. Therefore, vimentin positivity was deemed to be a characteristic of the thyroid gland rather than an epithelial-mesenchymal transition in carcinoma. Considering the vimentin positivity of normal follicular cells, we expected that the tumor cells forming small fol-

licles in this case would also be positive for vimentin. However, the tumor cells were positive for CK, but negative for vimentin. Therefore, these cells may also be derived from tumor cells rather than from the existing thyroid tissue.

The fibrous or myxoid material in the right tumor was stained for amyloid, which is frequently observed in C-cell carcinoma^{2, 5-7}. However, MT and amyloid staining revealed that these were not amyloids but fibrous or plasma components. Follicular cell carcinoma may be accompanied by abundant fibrotic components, which was consistent with this case⁵. Since red blood cells were also observed at the same site, these lesion areas may have been edematous because of the extravasation of fibrin and plasma components.

In the present case, tumor masses were found in areas corresponding to the thyroid glands on the left and right sides of the trachea. The gross features of both tumors were similar; however, their histological features differed. The tumor cells in the left tumor showed a predominant sheet-like growth pattern, while those in the right tumor were charac-

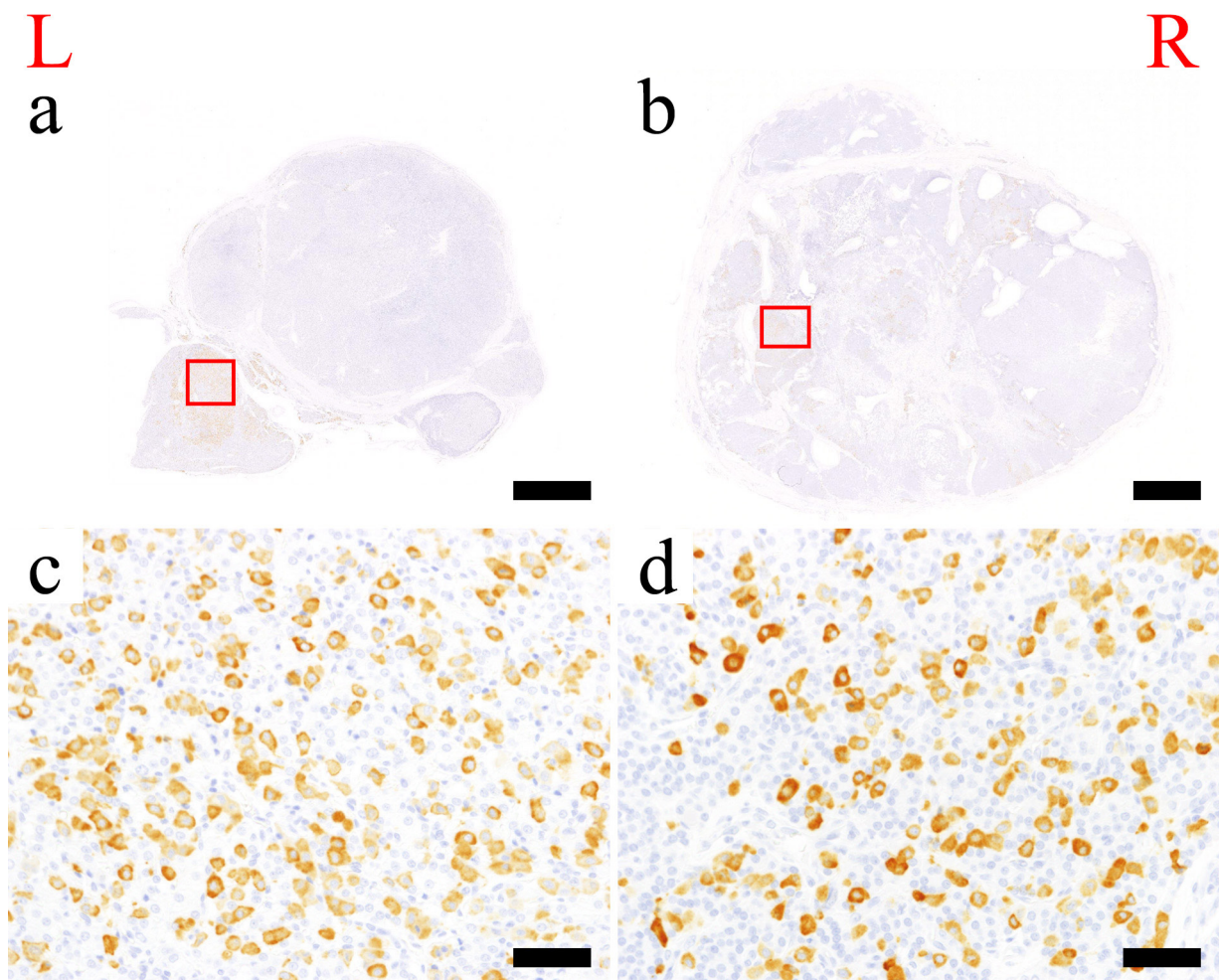


Fig. 6. Immunohistochemical staining for calcitonin. a and b) Loupe image of the left and right tumors. c and d) High magnification of the areas surrounded by squares in (a) and (b). C cells were positive for calcitonin and each C cell existed singly without forming clusters in both tumors. Bars=3 mm (a and b) and 50 μ m (c and d).

terized by dense areas with sheet-like growth of tumor cells, as in the left tumor, and sparse areas in which tumor cells formed small island-like nests or small follicles with abundant weak eosinophilic fibers or mucus-like material and microvessels in the stroma. Both tumors were diagnosed as malignant because of their capsular or vascular infiltration, although the degree of cellular atypia was relatively mild and mitotic figures were rarely observed. Immunostaining used to distinguish C-cell (medullary) carcinomas from parathyroid carcinomas, which are also characterized by a sheet-like growth pattern, demonstrated that most of the tumor cells in the sheet-like growth area in both tumors, as well as the tumor cells forming small follicles, were positive for thyroglobulin and negative for calcitonin and parathormone. Therefore, the tumor cells were determined to be derived from follicular cells of the thyroid gland. Although many thyroglobulin-negative cells were observed in the center of the sheet-like growth areas in both tumors, immunostaining for thyroglobulin has been reported to be weak in the compact cellular type of follicular cell carcinoma, and

negative cases have also been reported^{2, 5, 7, 19}.

In conclusion, based on immunohistochemical staining, ultrastructural results, and the predominance of sheet-like growth areas in both tumors, we diagnosed both tumors as thyroid follicular cell carcinomas of the compact cellular carcinoma subtype. The present case was characterized by the presence of many C cells in both tumors, making it difficult to differentiate them from C-cell carcinoma. Tumor cells were determined to be derived from existing C-cell complexes. To the best of our knowledge, this is the first report of electron microscopic findings and co-expression of CK and vimentin in thyroid follicular cell carcinoma in beagles.

Disclosure of Potential Conflicts of Interest: The authors declare no conflicts of interest.

Acknowledgments: We are grateful to Ayaka Yokoyama, Minami Kurahashi, and Yoshimi Tsukahara for their excellent technical assistance. This work was the result of using

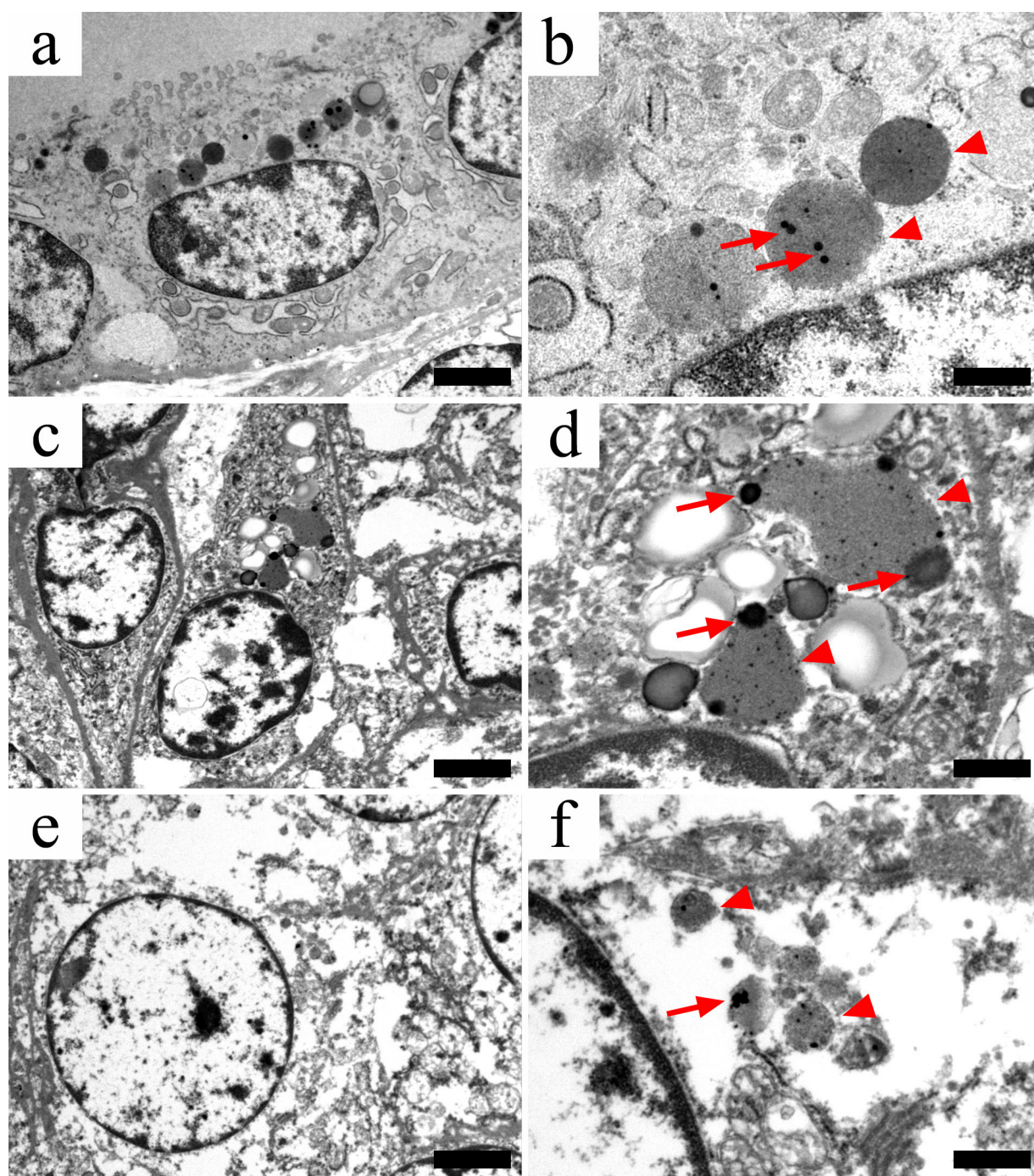


Fig. 7. Ultrastructural appearance of thyroid follicular cells. a and b) Thyroid follicular cells of a normal male 4-year-old beagle. c and d) Tumor cells in the sheet-like growth area. e and f) Tumor cells in the right tumor were large and had partially clear cytoplasm observed using the HE staining technique. b, d, and f) High magnification of (a), (c), and (e), respectively. Colloid droplets (arrowheads) and lysosomes (arrows), which are characteristic of thyroid follicular cells, were also seen in the tumor cells, although they were irregularly shaped or small compared with those in normal cells. Bars=2 μm (a, c, and e) and 500 nm (b, d, and f).

research equipment shared in the MEXT project to promote public utilization of advanced research infrastructure (program for supporting the construction of core facilities), Grant Number JPMX0440100022.

References

1. Wucherer KL, and Wilke V. Thyroid cancer in dogs: an update based on 638 cases (1995–2005). *J Am Anim Hosp Assoc.* **46**: 249–254. 2010. [[Medline](#)] [[CrossRef](#)]
2. Grant M. Jubb, Kennedy, and Palmer's Pathology of Domestic Animals, 5th ed. Elsevier, Philadelphia. 366–407.

- 2007.
3. Klein MK, Powers BE, Withrow SJ, Curtis CR, Straw RC, Ogilvie GK, Dickinson KL, Cooper MF, and Baier M. Treatment of thyroid carcinoma in dogs by surgical resection alone: 20 cases (1981–1989). *J Am Vet Med Assoc.* **206**: 1007–1009. 1995. [[Medline](#)] [[CrossRef](#)]
4. Théon AP, Marks SL, Feldman ES, and Griffey S. Prognostic factors and patterns of treatment failure in dogs with unresectable differentiated thyroid carcinomas treated with megavoltage irradiation. *J Am Vet Med Assoc.* **216**: 1775–1779. 2000. [[Medline](#)] [[CrossRef](#)]
5. Rosol TJ, Meuten DJ. Tumors of the endocrine glands. In: *Tumors in Domestic Animals*, 5th ed. DJ Meuten (ed). John Wiley & Sons, Ames. 791–815. 2017.
6. Campos M, Ducatelle R, Rutteman G, Kooistra HS, Duchateau L, de Rooster H, Peremans K, and Daminet S. Clinical, pathologic, and immunohistochemical prognostic factors in dogs with thyroid carcinoma. *J Vet Intern Med.* **28**: 1805–1813. 2014. [[Medline](#)] [[CrossRef](#)]
7. Leblanc B, Parodi AL, Lagadic M, Hurtrel M, and Jobit C. Immunocytochemistry of canine thyroid tumors. *Vet Pathol.* **28**: 370–380. 1991. [[Medline](#)] [[CrossRef](#)]
8. Okino H, Matsui S, Shioda S, Nakai Y, and Kurosumi K. Ultrastructural and morphometric studies on the rat pituitary thyrotrophs and thyroid follicular cells following administration of thyrotropin releasing hormone. *Arch Histol Jpn.* **42**: 489–505. 1979. [[Medline](#)] [[CrossRef](#)]
9. Paiement J, and Leblond CP. Localization of thyroglobulin antigenicity in rat thyroid sections using antibodies labeled with peroxidase or 125I-radioiodine. *J Cell Biol.* **74**: 992–1015. 1977. [[Medline](#)] [[CrossRef](#)]
10. Woicke J, Al-Haddawi MM, Bienvenu JG, Caverly Rae JM, Chanut FJ, Colman K, Cullen JM, Davis W, Fukuda R, Huisinga M, Walker UJ, Kai K, Kovi RC, Macri NP, Marxfeld HA, Nikula KJ, Pardo ID, Rosol TJ, Sharma AK, Singh BP, Tamura K, Thibodeau MS, Vezzali E, Vidal JD, and Meseck EK. International Harmonization of Nomenclature and Diagnostic Criteria (INHAND): Nonproliferative and proliferative lesions of the dog. *Toxicol Pathol.* **49**: 5–109. 2021. [[Medline](#)] [[CrossRef](#)]
11. Leblanc B, Paulus G, Andreu M, and Bonnet MC. Immunocytochemistry of thyroid C-cell complexes in dogs. *Vet Pathol.* **27**: 445–452. 1990. [[Medline](#)] [[CrossRef](#)]
12. Kameda Y. Co-expression of vimentin and 19S-thyroglobulin in follicular cells located in the C-cell complex of dog thyroid gland. *J Histochem Cytochem.* **43**: 1097–1106. 1995. [[Medline](#)] [[CrossRef](#)]
13. Kameda Y. The occurrence of a special parafollicular cell complex in and beside the dog thyroid gland. *Arch Histol Jpn.* **33**: 115–132. 1971. [[Medline](#)] [[CrossRef](#)]
14. Kameda Y, and Ikeda A. Immunohistochemical study of the C-cell complex of dog thyroid glands with reference to the reactions of calcitonin, C-thyroglobulin and 19S thyroglobulin. *Cell Tissue Res.* **208**: 405–415. 1980. [[Medline](#)] [[CrossRef](#)]
15. Kameda Y. Follicular cell lineage in persistent ultimobran- chial remnants of mammals. *Cell Tissue Res.* **376**: 1–18. 2019. [[Medline](#)] [[CrossRef](#)]
16. Takeshima K, Ariyasu H, Uraki S, Morita S, Furukawa Y, Inaba H, Iwakura H, Doi A, Warigaya K, Murata SI, Enomoto K, Hotomi M, and Akamizu T. False-positive staining of thyroglobulin distinguished from mixed medullary and follicular thyroid carcinoma by duplex in situ hybridization. *Endocr J.* **67**: 1007–1017. 2020. [[Medline](#)] [[CrossRef](#)]
17. Jankovic J, Tièche E, Dettwiler M, Hahn K, Scheemaeker S, Kessler M, Daminet S, Rottenberg S, and Campos M. Canine follicular cell and medullary thyroid carcinomas: immunohistochemical characterization. *Vet Pathol.* **61**: 524–533. 2024. [[Medline](#)] [[CrossRef](#)]
18. Miettinen M, Franssila K, Lehto VP, Paasivuo R, and Virtanen I. Expression of intermediate filament proteins in thyroid gland and thyroid tumors. *Lab Invest.* **50**: 262–270. 1984. [[Medline](#)]
19. Moore FM, Kledzik GS, Wolfe HJ, and DeLellis RA. Thyroglobulin and calcitonin immunoreactivity in canine thyroid carcinomas. *Vet Pathol.* **21**: 168–173. 1984. [[Medline](#)] [[CrossRef](#)]